Chemical Engineering Journal 165 (2010) 776–783

Contents lists available at ScienceDirect

Chemical Engineering Journal

journal homepage: www.elsevier.com/locate/cej

Residence time distribution and back-mixing in a tubular electrochemical reactor operated with different inlet flow velocities, to remove Cr(VI) from wastewater

S.A. Martínez-Delgadillo[a,*], H. Mollinedo-Ponce[b], V. Mendoza-Escamilla[c], C. Barrera-Díaz[d]

[a] Depto. Ciencias Básicas. Universidad Autónoma Metropolitana, Azcapotzalco, Av. San Pablo 180, Azcapotzalco CP 07740, México DF, Mexico
[b] SEPI-ESIME-Zacatenco IPN, Av. IPN s/n Unidad Profesional Adolfo López Mateos, México DF, Mexico
[c] Depto. Electronica. Universidad Autónoma Metropolitana, Azcapotzalco, Av. San Pablo 180, Azcapotzalco CP 07740, México DF, Mexico
[d] Centro de Investigación en Química Sustentable, UAEM, Carretera Toluca-Ixtlahuaca, km 14.5, San Cayetano de Morelos, Toluca, Mexico

ARTICLE INFO

Article history:
Received 23 August 2010
Received in revised form
28 September 2010
Accepted 29 September 2010

Keywords:
Electrochemical
CFD simulations
Hexavalent chromium
Tubular reactor
Back-mixing

ABSTRACT

In Mexico, the concentration of Cr(VI) in plating industries wastewater is well above Mexican environmental regulations (0.5 mg/L). The electrochemical Cr(VI) reduction, using iron electrodes has been an alternative process, which has been applied with success to remove Cr(VI) from wastewaters. However, few studies have been performed to evaluate the flow field behavior into the electrochemical reactors. In this work, tests at a novel tubular electrochemical reactor were performed. Five different inlet flow velocities with three different inlet positions (central, lateral and tangential inlets) were tested to evaluate their effect on the reactor performance. To study the flow field behavior throughout the reactor, CFD simulations were carried out. The results showed that at low inlet velocities, the reactor dispersion has strong dependence on the inlet position. On the other hand, when the reactor was operated at higher inlet velocities, the dispersion is reduced and presented similar values for the three reactor inlets. As a consequence of the dispersion reduction in the reactor, the residence time required to reduce the Cr(VI) concentration from 1000 mg/L to <0.5 mg/L, can be decreased until 20%.

© 2010 Elsevier B.V. All rights reserved.

1. Introduction

In Mexico, one of the most important water pollution problems is caused by plating industries. Only a very small quantity of these industries treats their wastewaters before discharging them to the sewage. In addition, when the wastewater is treated, the treatment normally consists of adjusting the pH to 7.0. The lack of treatment or its low efficiency, increases the concentration of heavy metals, such as Cr(VI), in the discharged wastewater, well above Mexican environmental regulations (0.5 mg/L) [1]. Cr(VI) is considered a very toxic heavy metal [2]. There are different available technologies to remove chromium(VI) from wastewaters (e.g. the use of bisulphite, evaporation, ion exchange, and ferrous sulphate, among others). These methods have some drawbacks such as the high inversion and operational costs that none of the small industries, the majority in Mexico, can afford. Moreover, these technologies require implementation of new infrastructure and generate large quantities of sludge, as in the case of using ferrous sulphate [3], which in turn raise the costs due to they have to be treated, handled and disposed. Electrochemical treatment is presented as an alternative method to reduce Cr(VI) in wastewaters to achieve low Cr(VI) concentration [4]. This treatment has been carried out with different electrode materials, for instance, carbon felt electrodes polypyrrole-coated aluminum electrodes or others [5–7]. However the treatment time is too long and in some cases the Cr(VI) concentration removed is quite low (about 50 mg/L). In this work carbon steel electrodes were used to remove Cr(VI) at high concentrations (1000 mg/L), because they have some advantages: electrode low costs, the water treated is recyclable and low amount of sludge are generated that contains chromite [8], which has refractory properties. During the electrochemical process, at the anode Fe(II) ions are released into solution, as shown in reaction (1).

$$Fe \rightarrow Fe^{2} + 2e^{-} \quad (1)$$

In the solution, the Cr(VI) is reduced to Cr(III) as a result of the Fe(II) to Fe(III) oxidation reaction, as shown in reaction (2).

$$6Fe^{2+} + Cr_2O_7^{2-} + 14H^{+} \rightarrow 6Fe^{3+} + 2Cr^{3+} + 7H_2O \quad (2)$$

Hydrogen gas is also released from the cathode during the process [16].

* Corresponding author.
E-mail addresses: samd@correo.azc.uam.mx (S.A. Martínez-Delgadillo), helviomollinedo@yahoo.com (H. Mollinedo-Ponce), mevx@correo.azc.uam.mx (V. Mendoza-Escamilla), cbd0044@yahoo.com (C. Barrera-Díaz).

1385-8947/$ – see front matter © 2010 Elsevier B.V. All rights reserved.
doi:10.1016/j.cej.2010.09.066

At industrial level, it is usually more profitable to operate continuous processes with reactors that achieve greater overall conversions, as plug flow reactors [9]. However, few studies to evaluate the behavior of velocity field throughout the electrochemical reactor operated with different configurations have been reported. In reactor design, one of the most important aspects to evaluate their performance requirements is to know with sufficient approximation the velocity field inside the vessel in order to predict its behavior [10]. In our previous study [11] different positions of the inlet reactor were evaluated while operating the reactor only at low inlet velocities. It was demonstrated that the inlet position had a considerable effect on the reactor flow field and the back-mixing degree or dispersion. This is important because the dispersion in the reactor has important an important effect on the reactor conversion and yield [12]. The present work extends the analysis considering five higher inlet flow velocities and evaluates their effect on the residence time and back-mixing into a novel tubular electrochemical continuous reactor, in laminar flow regime using state-of the-art CFD tools [13–15]. Due to the complex geometry of the reactor, the computational model was meshed using four nodes tetrahedral cells (Tet/Hybrid type TGrid). Several analyses of each reactor model with different mesh sizes were performed to obtain a grid independence solution and no significant changes occur in the solutions with a further mesh refinement of the models presented. Due to low operating fluid velocities, a laminar flow model was used in all cases. The simulation was carried out in steady state for each flow velocity inlet. Moreover, to obtain the exit age distribution curve and the dispersion at the different operation conditions, transient simulation was performed using the species transport equation to monitor the tracer concentration at the reactor exit. The dispersion effect was introduced in the model to describe the Cr(VI) reduction for the different operation conditions of the reactors.

2. Materials and methods

The electrochemical tubular reactor of carbon steel material, shown in Fig. 1, was used during the experimentations. The operation volume was 2.289 L and its dimensions were 1.05 m length and 0.054 m internal diameter (ID). Three reactor inlets were tested; lateral (L), central (C) and tangential (T). A central polished carbon steel rod measuring 1.05 m served as cathode, giving a 0.0094 m^2 cathode surface area. A 3.0 m length spiral wire of the same material and ID, which served as the anode with a surface area of 0.05654 m^2, was isolated from the cathode by rubber gaskets. The electrochemical reactor was fed with a peristaltic pump and the flow rate was changed to regulate the different flow velocity inlets. It was supposed that the electrochemical reactor was a closed vessel. Eq. (1) was used to evaluate the mean residence time and Eq. (2) to evaluate the N_d. The radial mixing was not considered because in streamline flow of fluids through pipes, axial mixing is mainly due to fluid velocity gradients and this method is reliable to use when $N_d < 1$ [9].

$$\mathtt{th} = \frac{\int_0^\infty tCdt}{\int_0^\infty Cdt}$$

$$\frac{\sigma^2}{\mathtt{th}} = 2\left(\frac{D}{uL}\right) - 2\left(\frac{D}{uL}\right)^2 (1 - e^{(uL/D)})$$

where t, time (min); C, tracer concentration (mg/L); σ^2, variance (min^2), th, mean residence time (min), D, dispersion coefficient

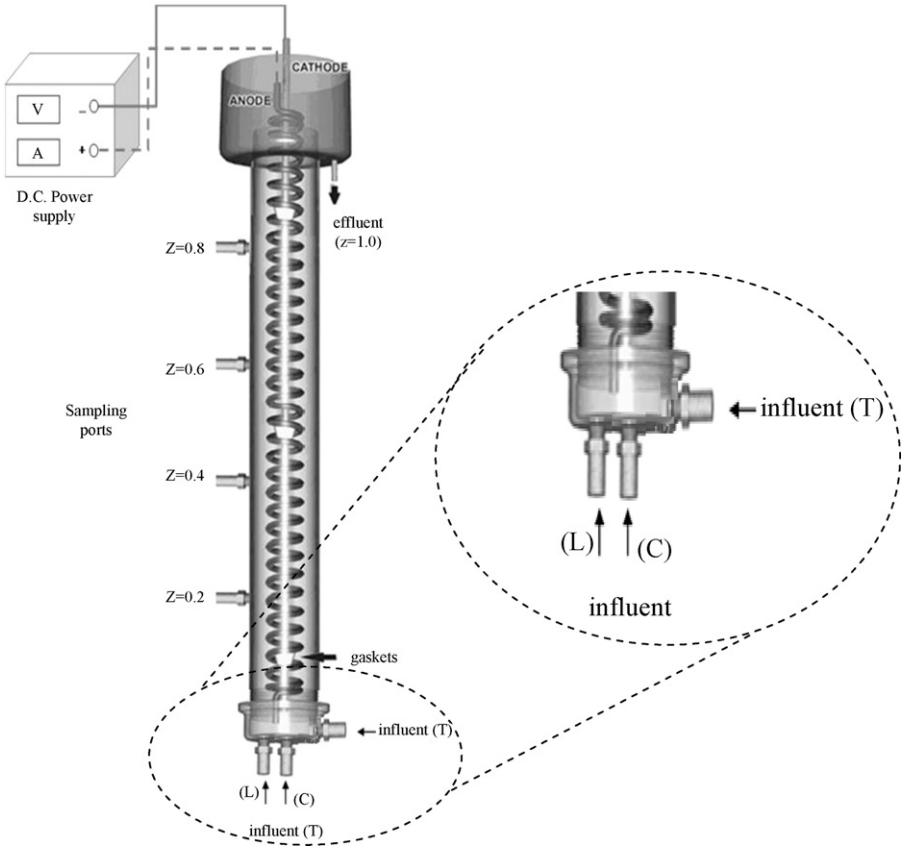

Fig. 1. The schematic diagram of the electrochemical tubular reactor.

($m^2\ s^{-1}$), u, flow velocity (m/s), L, reactor length (m), **E**, exit age distribution function (min^{-1}), θ, t/th (dimensionless) and the dispersion number $N_d = D/uL$.

To obtain the residence time to reduce the Cr(VI) from 1000 mg/L to 0.5 mg/L at influent pH = 0.5 in the electrochemical reactor a experimental validated model, with the dispersion effect included, was used [10]. The Cr(VI) removal in the tubular reactor is described by Eq. (3).

$$\mathrm{th}\frac{\partial \mathrm{Cr}}{\partial t} = \frac{D}{uL}\frac{\partial^2 \mathrm{Cr}}{\partial z^2} - \frac{\partial \mathrm{Cr}}{\partial z} - \mathrm{th}\frac{k_1 \mathrm{Cr}}{1 + k_2 \mathrm{Cr}} \tag{3}$$

and the boundary conditions [17] are shown in Eqs. (4) and (5).

$$\mathrm{Cr} - \frac{D}{uL}\frac{\partial \mathrm{Cr}}{\partial z} - \mathrm{Cr_o} = 0 \quad \text{at } z = 0 \tag{4}$$

$$\frac{\partial \mathrm{Cr}}{\partial z} = 0 \quad \text{at } z = 1 \tag{5}$$

where Cr, Cr(VI) concentration in the reactor (mg dm^{-3}); $\mathrm{Cr_o}$, influent Cr(VI) concentration (mg dm^{-3}); k_1, constant rate of Cr(VI) removal (min^{-1}); k_2, constant rate of Cr(VI) removal ($dm^3\ mg^{-1}$); x, across position in the reactor (m); t, time (min); th, hydraulic residence time (min); and z, x/L (dimensionless).

The wastewater pH used in this work was 0.5 that remains almost constant during the electrochemical process avoiding the formation of iron and chromium insoluble species [16].

Fluent version 6.3 has been used to perform the CFD simulations at the steady (fully developed flow) and unsteady state fluid flow (species transport); a pressure-based segregated algorithm solver has been used, where the governing equations are solved sequentially. For the pressure–velocity coupling a non linear procedure called semi-implicit pressure-linked equation (SIMPLE) algorithm was used, for pressure discretization the Standard scheme was selected, and for the momentum discretization, the Second Order

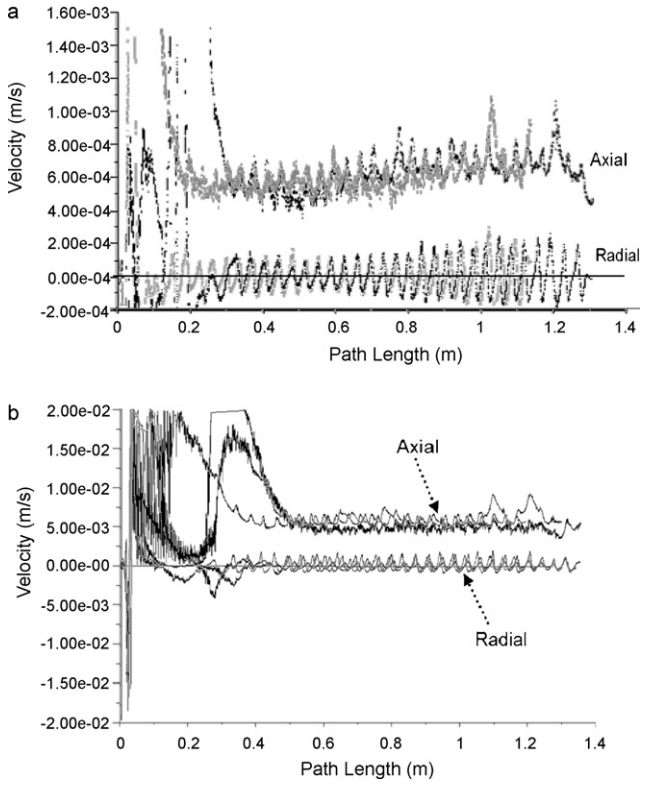

Fig. 2. Axial and radial velocity of different particles as a function of the path length, operating the reactor at: (a) 0.0481 m/s and (b) 0.388 m/s inlet flow velocities.

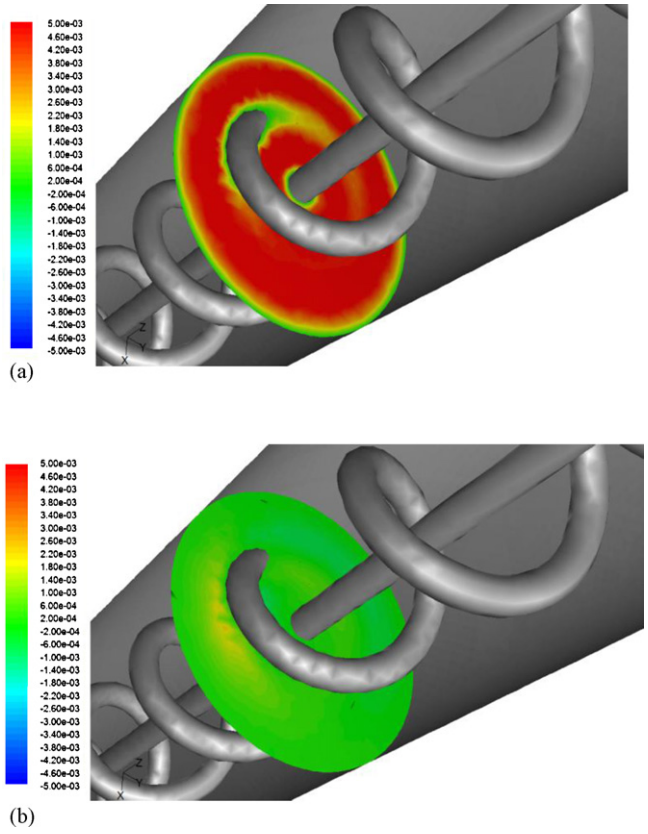

Fig. 3. Axial (a) and radial (b) velocity contours of the surface into the reactor, swept along z axis.

Upwind scheme was used. Once the steady state was obtained, transient simulation was performed using the species transport equation, then a pulse (lasting 5 s) of tracer with the same material properties as the working fluid and a concentration of unity was injected at the inlet surface; after the solution converged the tracer concentration was returned to zero again to simulate a pulse injection. The concentration of the tracer is monitored at the outlet and the age distribution function (**E**) and the dispersion number (N_d) were evaluated.

For the steady state flow simulation, the mass and momentum conservation equations are used and they are given respectively by Eqs. (6) and (7).

$$\nabla \vec{v} = 0 \tag{6}$$

$$\nabla(\rho \vec{v}\vec{v}) = -\nabla p + \nabla(\bar{\tau}) + \rho\vec{g} + \vec{F} \tag{7}$$

where $\vec{v}$, velocity vector; ρ, density; $\bar{\tau}$, stress tensor; $\rho\vec{g}$, gravitational body force; $\vec{F}$, external force vector.

For the tracer injection, unsteady state simulations were performed and the conservation equations for transport species were used Eq. (8).

$$\frac{\partial}{\partial t}(\rho Y_i) + \Delta(\rho \vec{v} Y_i) = -\Delta(\vec{J}_i) \tag{8}$$

where Y_i is the local mass fraction of species i, J_i is the diffusion flux of species i. considering that diffusion is caused by the concentration gradient, J_i is given by Eq. (9).

$$\vec{J}_i = -\rho D_{i,m} \nabla Y_i \tag{9}$$

where $D_{i,m}$ is the diffusion coefficient for species i.

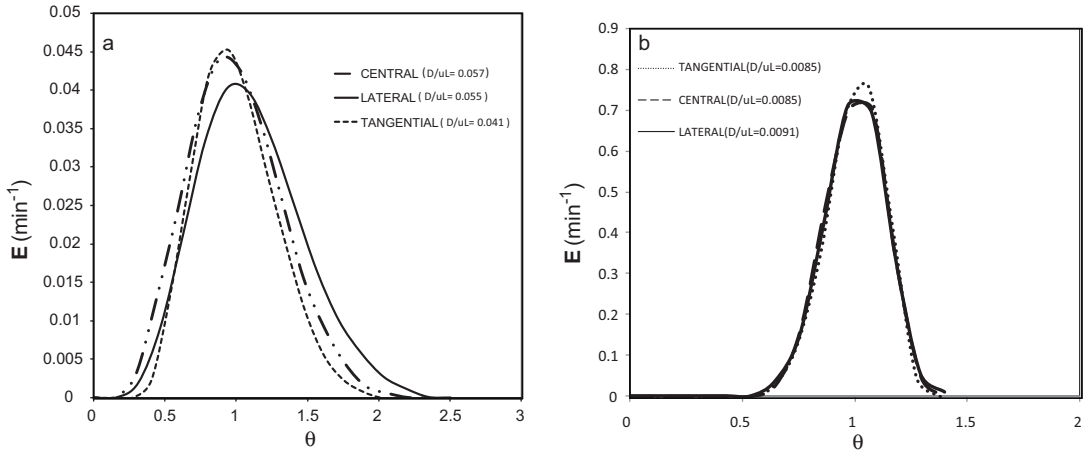

Fig. 4. The exit age distribution curve **E** at the electrochemical reactor for each inlet and influent velocity rate: (a) the lowest velocity (0.0481 m/s) and (b) the highest velocity (0.388 m/s).

3. Results and discussion

In this work, the age distribution function (**E**) and the dispersion number (N_d) was evaluated for the different inlet flow velocities and reactor inlets. Fig. 2 shows the axial and radial velocity as a function of the path length for different particles, when the electrochemical reactor with tangential inlet was operated at the lowest (0.0481 m/s) and the highest (0.388 m/s) inlet flow velocities. The particle track plots of the other velocities and inlets are not presented, because the results were in between.

In both cases, the radial velocity of the particles is high only at the zone near the reactor inlet due to the "end effects". The dark blue zone near the reactor inlet in Fig. 7 shows the extent of the inlet zone for the reactor operated at the different inlets. Above this inlet zone, the radial velocities are lower than the axial velocities, and their values are about 13–16% of the axial velocity, for the lowest (0.0481 m/s) and the highest (0.388 m/s) inlet flow velocities, respectively. These percentage values (%) are much lower than those reported in other study carried out in bubble columns, where the radial velocity was about 36% of the axial velocity. In addition, the dispersion value of the radial dispersion coefficient reported was typically about 1% of the value of the axial dispersion [18]. Based on these results, the dispersion model used in the present work is appropriated because the reactor presents a relatively poor radial mixing compared to the axial mixing. Fig. 3 shows the axial and radial velocity contours of the surface into the reactor swept along *z* axis. As seen, the axial velocity is much higher than the radial velocity. The radial velocity has small increments only around the anode (helical).

During the electrochemical process hydrogen gas is generated on the cathode and the bubble hydrogen gas rise velocity, u_b is given by Eq. (10) [19].

$$u_b = u_G + u_L + u_O \tag{10}$$

where u_G and u_L are the superficial velocities of gas and liquid respectively, and u_O is the rise velocity of a single bubble in a quiescent electrolyte. Based on the highest current used (5.0 A), 6.22933E−07 m^3/s of hydrogen gas are generated, then u_G = 0.000272 m/s. The mean superficial velocities liquid (u_L) evaluated in the reactor operating at 0.0481 and 0.388 m/s inlet velocities were, 0.0007486 and 0.0046142 m/s, respectively. The diameters of the hydrogen bubbles are small and spherical in shape, with a diameter in the range of 50–200 μm and the u_O is 0.0020 and 0.0109 m/s, respectively [20]. Based on a bubble diameter of 200 μm, the u_b calculated for the 0.0481and 0.388 m/s inlet flow velocities, are 0.0119 and 0.0158 m/s, respectively. Then u_b is 6% and 29% higher than u_L, respectively. It means that the dispersion and the residence time are almost unaffected because the liquid at those relatively high velocities, removes the bubbles from cathode surface, dispersing them into the fluid reducing the turbulence promoting effect of the bubbles, in agreement with the result in other work [19], where percentages of 5–25% were reported. In the same work, the radial mixing is considered important when u_b 40–200% higher than u_L because the bubbles may cause turbulent eddies increasing the dispersion in the reactor.

Fig. 4(a) and (b) shows the results of the age distribution function obtained for the lowest (0.0481 m/s) and the highest (0.388 m/s) inlet flow velocities for the three reactor inlets. As seen, there are differences in the age distribution function (**E**) when the electrochemical reactor is operated at the lowest influent flow velocity (Fig. 4(a)). In this case, the curve with the tangential inlet is the most symmetrical, while the curve with the highest deviation from the plug flow behavior was obtained when the reactor was operated with the central inlet. As shown, the curves obtained operating the reactor with lateral and central inlets, show that at these conditions the reactors have more short-lived material leaving the electrochemical reactor, than when the reactor is operated with tangential inlet, which affects the conversion rate in the reactor. On the other hand, at the highest inlet flow velocity (Fig. 4(b)) there are no important differences among the age distribution function (**E**) of the three different inlets.

Fig. 5(a) shows the dispersion number (N_d) obtained at different influent flow velocities. As shown, the N_d is reduced as the influent velocity increases and for inlet velocities higher than 0.15 m/s, there was not important reduction in the dispersion. In addition, operating the reactor with the tangential inlet and with inlet velocities lower than 0.15 m/s, the dispersion in the reactor is the lowest of the three inlets. At higher inlet velocities than that value, the dispersion is similar with the three inlets. Fig. 5(b) shows that the ratio of the mean residence time (`th`), obtained with the exit age distribution curve, to the residence time (`tm`) measured experimentally (ratio of reactor operation volume/flow rate) has a value higher than 1.0, only at a flow inlet of 0.0481 m/s with the central inlet position the ratio value is 1.0. This means that due to the electrodes configuration, the liquid particles travel in a non-straight line due to the helical shape of the anode, as seen clearer in Fig. 6(a), where the some particle traces along the reactors are shown. In addition, in Fig. 2 it is shown that the path length of the particles is higher than the reactor length (1.05 m). This is significant because the reactor seems to have an "extra" volume, which

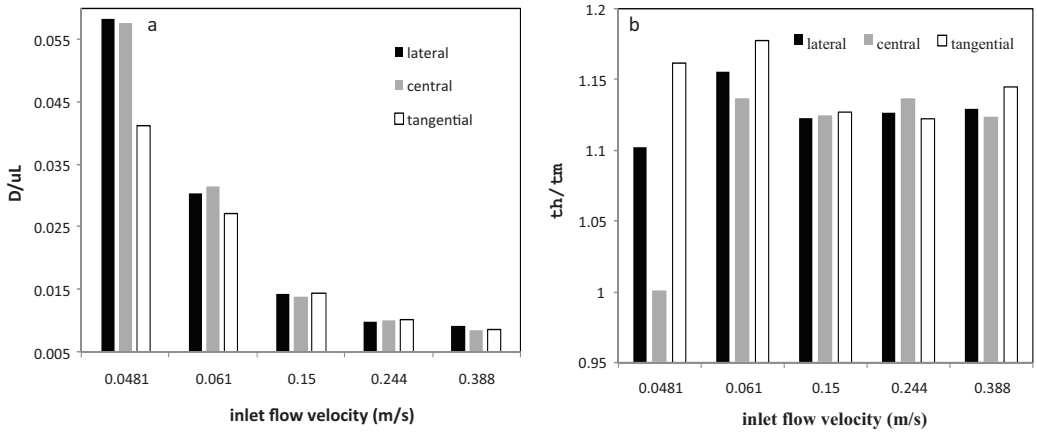

Fig. 5. (a) N_d and (b) ratio residence time mean to measured (th/tm) at different inlet flow velocities in the electrochemical reactor.

reaches until 12% in the most cases and more than 15% in the case of the reactor operated with tangential inlet and with influent velocities of 0.0481 and 0.061 m/s. Moreover, the axial and radial velocity of the particles is not constant along the reactor (as seen in Fig. 2), near the inlet the velocities are the highest, but after the first part of the reactor, their velocity is considerably reduced. Close to the anode, the particle traces and their velocities are affected due to its electrode helical shape, causing the velocity oscillations (Figs. 2 and 6(a)). This effect allows the reactants have more probability to react into the electrochemical reactor and the velocity oscillations around the electrodes cause an increase in the vorticity, as seen in Fig. 6(b), improving the mass transfer between the electrodes and the liquid without important increasing of the dispersion in the reactor.

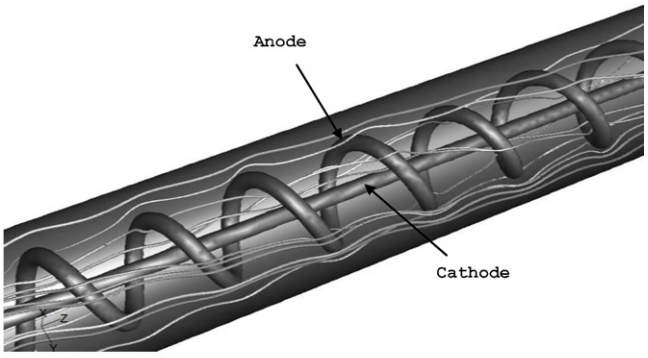

(a)

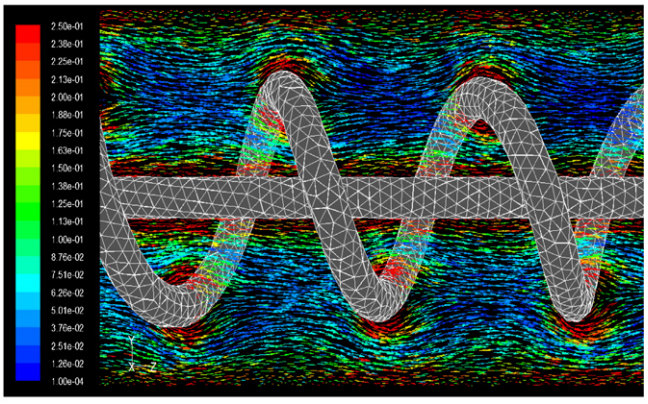

(b)

Fig. 6. (a) Particle traces into the electrochemical reactor and (b) velocity vectors colored by vorticity magnitude (1/s).

Fig. 7 shows the contours of axial velocity of the reactors operated with different flow velocities and reactor inlets. As seen, when the reactors with different inlets are operated at the lowest inlet flow velocity of 0.0481 m/s, a more homogeneous distribution of the axial velocity is reached with the tangential inlet, which explains why this configuration presented the lowest dispersion of the three inlets. The axial velocity contours into the reactor operated with the other two inlets (lateral and central); show zones with low and high axial velocities that cause fluctuations due to the no homogeneous flow velocity distribution that produces higher dispersion in the rector. Comparing the reactors operated with lowest (0.0481 m/s) and highest (0.388 m/s) inlet flow velocities, the contours show that at the highest inlet flow velocity, the axial velocity distribution fields in the three reactors are more homogeneous than at lower inlet flow velocities. Only in the first part of the reactor ("end effects"), there are zones of negative and higher positive axial velocity values, more extended in the reactor with lateral inlet, but beyond that zone, the flow velocity is reduced and the fluid streams are more uniform, mainly at inlet velocities of 0.15 m/s and higher, which also produces similar th/tm ratios, as seen in Fig. 5(b). This effect can be explained by the inertial forces of the fluid that create a velocity more regular profile, reducing the differences among the flow velocities, and then dispersion in the reactor. The higher vorticity and velocities of the fluid near the central electrode (cathode), cause the evolved bubble gas (H_2) are taken away so fast, dispersing them and avoiding that their size increases. Therefore, the coalescence effect is diminished and then the difference between u_b and u_L is reduced. Therefore, the effect of the bubble gas evolved on the dispersion was neglected, as it was mentioned before.

In Fig. 8 are shown the axial velocity profiles at reactor exit operated at low (a: left side) and high (b: right side) inlet flow velocity, with the three inlets. As seen, the axial velocity profiles have a pick of higher velocities when the reactor is operated at the low inlet flow velocity. On the other hand, the axial velocity exit profiles are more uniform at the highest inlet flow velocities. This effect is similar for the different inlets; it means that as the inlet flow velocity increases, the reactor dispersion decreases. The back-mixing has a strong influence on the reactor performance; hence, some authors have proposed alternatives to reduce it [21,22]. Increasing the flow velocity could be another alternative to reduce reactor dispersion that should be more studied. Table 1 shows the residence time to reduce the Cr(VI) concentration in the influent from 1000 mg/L to 0.5 mg/ L at the five inlet flow velocities and the three reactor inlets.

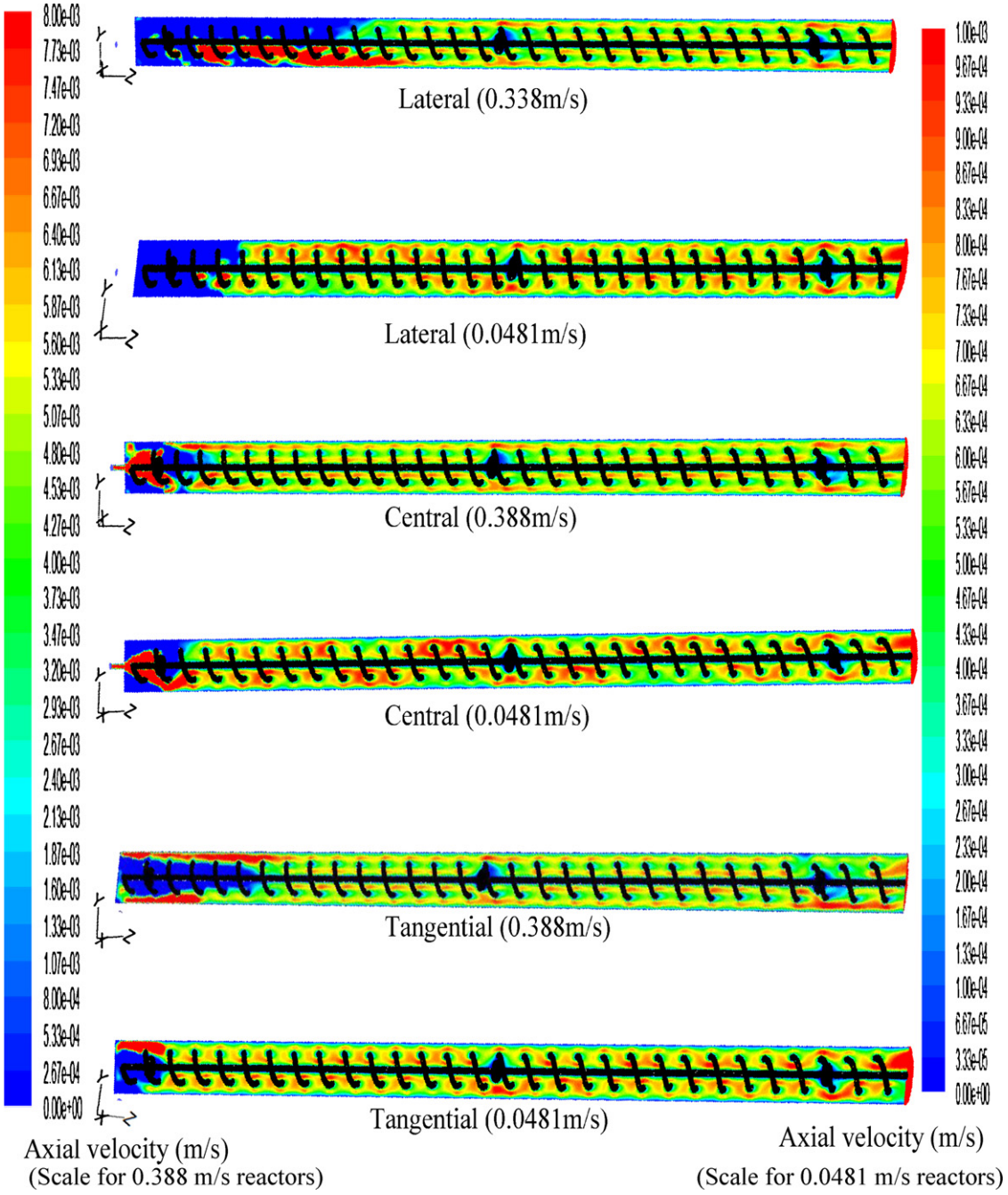

Fig. 7. Contours of axial velocity of the reactors operated with different inlets and inlet flow velocity.

Table 1
Residence time to reduce the Cr(VI) from 1000 mg/L to 0.5 mg/L at influent pH = 0.5 in the electrochemical reactor operated with different inlet flow velocities, reactor inlets and at different N_d.

Inlet flow velocity (m/s)	Residence time (min)		
	Central	Lateral	Tangential
0.0481	37	36.8	34
0.061	32.2	32.5	31.8
0.15	29.8	29.8	29.8
0.244	29.9	29.9	29.9
0.388	28.8	28.6	28.6

As seen, as the inlet flow velocity increases, the residence times are reduced because the dispersion in the reactor (Fig. 5(a)) is reduced. Moreover, at the lower inlet flow velocities (0.0481 and 0.061 m/s) the inlet type of reactor affects the dispersion and then the residence time (e.g. with the tangential inlet the N_d and the residence time are the lowest of the three inlets). On the other hand, at higher inlet flow velocities (0.15–0.388 m/s) the dispersion in the reactor is reduced as the inlet flow velocity increases, but its value is almost the same at the three reactor inlets. Then, at the highest inlet flow velocity (0.388 m/s) the residence time can be reduced until 20% in comparison with the reactor operated with a lateral inlet and the lowest (0.0481 m/s) influent velocity. This has an important effect on the operational costs of the process because the energy consumption can be reduced.

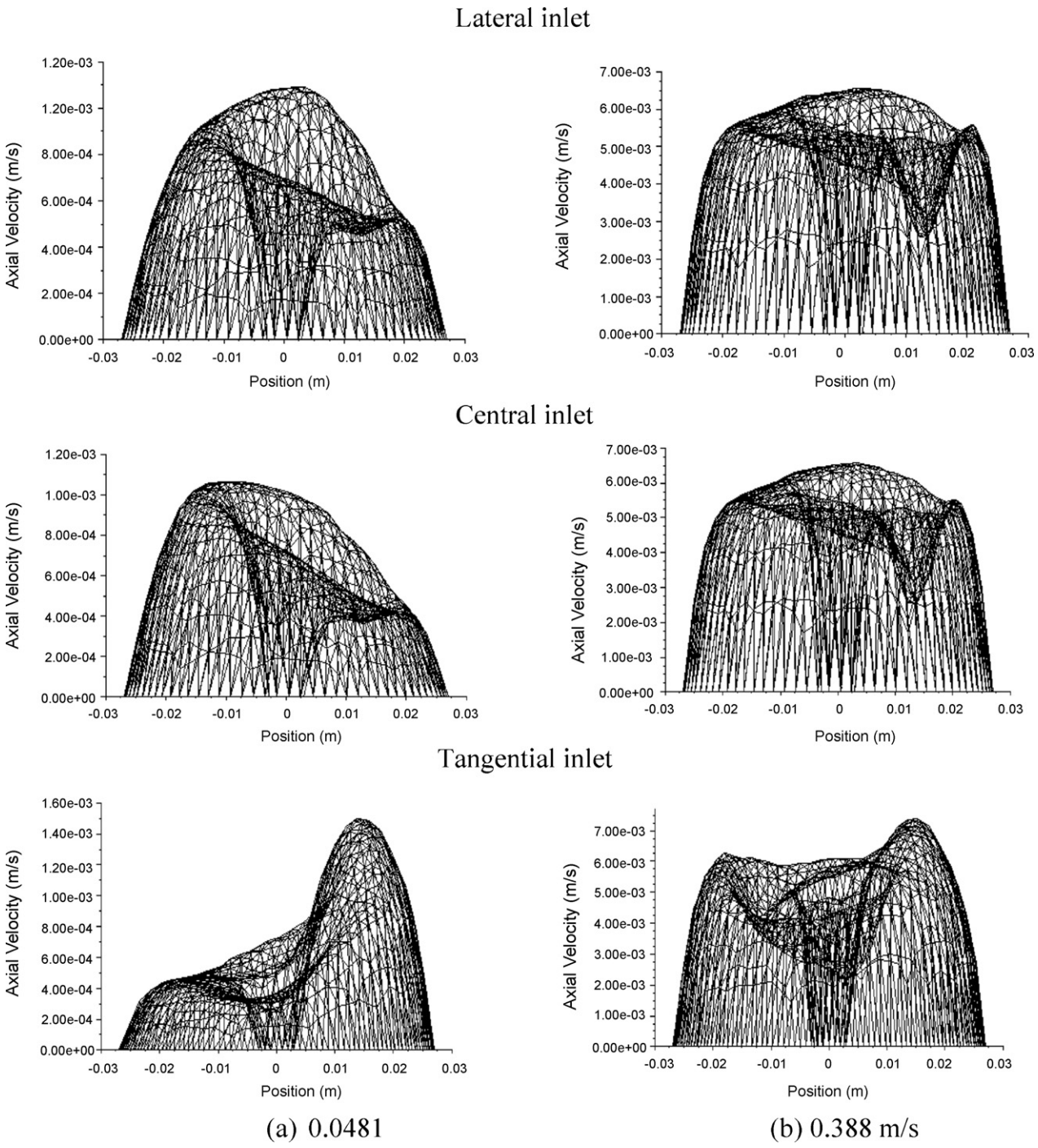

Fig. 8. Axial velocity profiles at exit of the reactor with different inlets at low (a) and high (b) inlet flow velocity.

4. Conclusions

Using computational fluid dynamics (CFD) simulations, it is possible to evaluate the hydrodynamic behavior inside the electrochemical reactor. At lower inlet flow velocities (<0.15 m/s), the dispersion is higher than at higher (≥0.15 m/s) inlet flow velocities. The type of the reactor inlet affects the dispersion when the reactor is operated at lower inlet flow velocity. On the other hand, at higher inlet flow velocity the dispersion in the electrochemical reactor, operated at the three reactor inlets, is almost the same. At the operational conditions, the dispersion in the electrochemical reactor is not affected by evolved gas from the cathode. The dispersion in the reactor is reduced at the high inlet flow velocities and its performance is improved, reducing the residence time until 20%, to remove the Cr(VI) concentration from 1000 mg/L to <0.5 mg/L.

References

[1] SEMARNAP, Nom-001-Ecol-1996, Diario Oficial de la Federación, México, 1997.
[2] U.S. Department of Health and Human Services, Chromium toxicity, Agency for Toxic Substances and Disease Register. Division of Health Education and Promotion. Course: SS3048, 2000.
[3] W. Eckenfelder, Industrial Water Pollution Control. Environmental Engineering Series, McGraw Hill, 2000.

[4] S.A. Martínez, M.G. Rodríguez, Removal of chromium hexavalent from rinsing chromating waters electrochemical reduction in a laboratory pilot plant, Water Sci. Technol. 49 (2004) 115–122.
[5] P. Rana, N. Mohan, C. Rajagopal, Electrochemical removal of chromium from wastewater by using carbon aerogel electrodes, Water Res. 38 (2003) 2811–2820.
[6] I. Frenzel, H. Holdik, V. Barmashenko, D.F. Stamatialis, M. Wessling, Electrochemical reduction of dilute chromate solutions on carbon felt electrodes, J. Appl. Electrochem. 36 (2006) 323–332.
[7] K.G. Conroy, C.B. Breslin, Reduction of hexavalent chromium at a polypyrrole-coated aluminium electrode: synergistic interactions, J. Appl. Electrochem. 34 (2004) 191–195.
[8] N. Kongsrichroern, C. Polprasert, Electrochemical precipitation of chromium (Cr(VI)) from an electroplanting wastewater, Water Sci. Technol. 31 (1995) 109.
[9] P. Trinidad, F. Walsh, Conversion expressions for electrochemical reactors which operate under mass transport controlled reaction conditions, part I: Batch reactor, PFR and CSTR, Int. J. Eng. Ed. 14 (1998) 431–441.
[10] O. Levenspiel, Chemical Reaction Engineering, 3rd ed., John Wiley, New York, 1999.
[11] S.A. Martínez-Delgadillo, H.R.P. Mollinedo, V.M. Gutiérrez, D.I. Barceló, J.M. Méndez, Performance of a tubular electrochemical reactor, operated with different inlets, to remove Cr(VI) from wastewater, Comput. Chem. Eng. 34 (2010) 491–499.
[12] K. Ekambara, J.B. Joshi, Axial mixing in laminar pipe flows, Chem. Eng. Sci. 59 (2004) 3929–3944.
[13] A.V. Atilano, H.F. Meier, J.J. Iess, M. Mori, Computational fluid dynamics (CFD) analysis of cyclone separators connected in series, Ind. Eng. Chem. Res. 47 (2008) 192–200.
[14] F. Schonfeld, S. Hardt, Simulation of helical flows in microchannels, AIChE J. 50 (2004) 771–778.
[15] J.M. Zalc, E.S. Szalai, M.M. Alvarez, F.J. Muzzio, Using CFD to understand chaotic mixing in laminar stirred tanks, AIChE J. 48 (2002) 2124–2134.
[16] M.G. Rodriguez, S.A. Martinez, Removal of Cr(VI) from wastewaters in a tabular electrochemical reactor, J. Environ. Sci. Health A: Environ. Sci. Eng. Toxic Hazard. A40 (2005) 2215–2225.
[17] P.V. Danckwerts, Continuous flow systems. Distribution of residence times, Chem. Eng. Sci. 2 (1953) 1–13.
[18] F. Camacho Rubio, A. Sánchez Mirón, M.C. Cerón García, F. García Camacho, E. Molina Grima, Y. Chisti, Mixing in bubble columns: a new approach for characterizing dispersion coefficients, Chem. Eng. Sci. 59 (2004) 4369–4376.
[19] W.S. Wu, G.P. Rangaiah, Effect of gas evolution on dispersion in and electrochemical reactor, J. Appl. Electrochem. 23 (1993) 113–119.
[20] N.P. Brandon, G.M. Kelsall, J. Appl. Electrochem. 15 (1985) 475.
[21] S.D. Sandesh, M.J. Sathe, J.B. Joshi, Residence time distribution and flow patterns in the single-phase annular region of annular centrifugal extractor, Ind. Eng. Chem. Res. 48 (2009) 37–46.
[22] S.S. Deshmukh, S. Vedantam, J.B. Joshi, S.B. Koganti, Computational flow modeling and visualization in the annular region of annular centrifugal extractor, Ind. Eng. Chem. Res. 46 (2007) 8343.